Available online at www.sciencedirect.com

ScienceDirect

Advances in Space Research 57 (2016) 309–319

ADVANCES IN SPACE RESEARCH (a COSPAR publication)

www.elsevier.com/locate/asr

Modulation of total electron content by global Pc5 waves at low latitudes

E. Vorontsova [a], V. Pilipenko [b,c,*], E. Fedorov [b], A.K. Sinha [d], G. Vichare [d]

[a] Research Station of Russian Academy of Sciences, Bishkek, Russian Federation
[b] Space Research Institute, Moscow, Russian Federation
[c] Institute of Physics of the Earth, Moscow, Russian Federation
[d] Indian Institute of Geomagnetism, Mumbai, India

Received 13 July 2015; received in revised form 28 October 2015; accepted 28 October 2015
Available online 3 November 2015

Abstract

Earlier studies have successfully demonstrated that the GPS–TEC technique is a powerful method to study the propagation pattern of transient disturbances in the ionosphere. This technique has turned out to be sensitive enough to detect ionospheric signatures of ULF waves as well, particularly at high latitudes. It has already been reported earlier that during the recovery phase of the strong magnetic storm on Oct. 31, 2003, intense Pc5 geomagnetic activity was accompanied with distinct pulsations of the same periodicity in the TEC data from high-latitude GPS receiving stations. The present study reveals the identical features in geomagnetic and TEC data at low-latitude stations in the Indian sector as well. However, the presented observational results on TEC modulation by global Pc5 waves at low latitudes cannot be interpreted on the basis of the Alfven mode concept. The most promising mechanism that can explain the present observations is the plasma compression by fast magnetosonic mode. Theoretical order-of-magnitude estimates of the ratio between pulsation amplitudes in TEC and geomagnetic field based on the proposed mechanism is found to be about the same as the observed values.

Keywords: ULF waves; GPS/TEC; Low latitude; Ionosphere

1. Introduction

The terrestrial ionosphere represents an inner boundary of the space environment where the transfer of energy through the coupled magnetosphere–ionosphere–atmosphere system takes place. The ionosphere can be imagined as a thin film of the ionized gas stretched over the globe, and this film is very sensitive to impacts from above and below. The ever-growing facilities of navigation global satellite system (GPS) provide information on variations of a radiopath-integrated ionospheric parameter – the total electron content (TEC). GPS/TEC observations have emerged as a global technique to monitor the propagation of waves and transients in the ionosphere (Komjathy et al., 2012). This is the reason for wide interest to use ionospheric observations with the use of the global positioning system (GPS) to monitor tsunami propagation (Galvan et al., 2011), to detect distant explosions (Fitzerald, 1997), to reveal the earthquake precursory (Liu et al., 2004; Zakharenkova et al., 2008) and post-seismic signatures (Tsai et al., 2011), etc. The ionosphere is also under the permanent impact from various space weather

* Corresponding author at: Space Research Institute, Profsojuznaja 84/32, Moscow 117997, Russia.
E-mail addresses: voroncova_e@mail.ru (E. Vorontsova), pilipenko_va@mail.ru (V. Pilipenko), enfedorov1@yandex.ru (E. Fedorov), sinha.ashwini@gmail.com (A.K. Sinha), vicharegeeta@gmail.com (G. Vichare).

http://dx.doi.org/10.1016/j.asr.2015.10.041
0273-1177/

disturbances. Using the technique introduced by Saito et al. (1998), GPS-derived TEC has been extensively used to characterize traveling ionospheric disturbances (TIDs) of different nature, including space weather related disturbances, at middle (Tsugawa et al., 2007) and high (Van de Kamp et al., 2014) latitudes. The interaction between the solar wind and the magnetosphere provides a rich source for various types of ultra-low-frequency (ULF) waves, which are always present in the magnetosphere and perturb its inner boundary, the ionosphere. Local variations of ionospheric electron density caused by long-period ULF waves (Pc3–5, Pi2–3) can be detected by modern ground-based sounding techniques: HF Doppler sounders (Menk et al., 2007), SuperDARN radars (Teramoto et al., 2014), transionospheric radiowave propagation (Sinha et al., 2001), riometers (Spanswick et al., 2005), etc. The TEC technique is sensitive enough to detect at least some types of ULF waves in the ionosphere: Pc5 waves at high latitudes (Pilipenko et al., 2014a,b; Watson et al., 2015) and Pc3–4/Pi2 waves at middle (Davies and Hartman, 1976; Hamada et al., 2015) latitudes.

So far, the effect of TEC modulation by ULF waves is not well understood and is still a challenge for the MHD wave theory. Observations have revealed that the relative disturbance of TEC by Pc3 waves is about the same or even larger than that of geomagnetic field (Skone and Nicholson, 2006). Also, in the high-latitude Pc5 event of Oct. 31, 2003 analyzed by Pilipenko et al. (2014a,b) the relative amplitude of TEC variations, $\Delta N_T/N_T \sim 2.5\%$, was larger than that of geomagnetic pulsations, $\Delta B/B \sim 1\%$. Various proposed TEC modulation mechanisms (Poole and Sutcliffe, 1987; Waters et al., 2007; Pilipenko et al., 2014a,b), were based on different aspects of the Alfven wave interaction with the high-latitude ionosphere. In general, Pc5 pulsations are localized at auroral latitudes, and are the eigenmodes of Alfven field line oscillations between the conjugate ionospheres.

However, there are specific global Pc5 waves which are about an order of magnitude more intense than common Pc5 pulsations. They are observed in the recovery phases of geomagnetic storms during high solar wind streams (Rae et al., 2005; Potapov et al., 2006). The reason for such outstanding intensity has not been firmly established yet. Global Pc5 waves are not confined only to auroral latitudes, but they are extended deep into the magnetosphere and can be observed even at equatorial latitudes. The large latitudinal range of global Pc5 pulsations cannot be interpreted based on the theory of field line Alfven resonance excitation, because this mechanism provides a latitudinally localized wave structures. Moreover, global Pc5 waves do not show typical features of resonant structure: latitude-dependent spectral peaks and phase gradient. Marin et al. (2014) indicated that the observed Pc5 oscillations at low and equatorial latitudes are not due to evanescent surface-like mode at the magnetopause, but could be a result of different wave transmission mechanism, probably the MHD waveguide mode. Motoba et al. (2002) suggested that the penetration of global Pc5 waves towards the Earth's equator was caused by a nearly instant propagation of electromagnetic disturbance in the Earth-ionosphere waveguide with velocity about the light speed.

In this paper, we consider an example of global Pc5 waves excited during the recovery phase of Oct. 31, 2003 storm, and demonstrate that the standard TEC/GPS technique is sensitive enough to detect intense Pc5 geomagnetic pulsations at low latitudes. We also discuss possible physical mechanisms of TEC fluctuations associated with these waves.

2. Observational information and data processing

Magnetometer data from the meridional array along the geomagnetic longitude $\Lambda \sim 150°$ (local noon ~7 UT) extending from mid-latitude station Bishkek (Kyrgyzstan) across India up to the dip equator are used (Fig. 1). Their coordinates are given in Table 1.

The GPS technique provides the means to estimate the slant TEC variations N_T on the basis of phase measurements of two-frequency, f_1 and f_2, GPS receivers using the widely-used relationships from (Hofmann-Wellenhof et al., 1992; Afraimovich et al., 2013). We have used these relationships without differential code biases. The slant TEC can be converted into vertical vTEC at the pierce point (intersection of radiopath with the ionosphere maximum) using the formula from Klobuchar (1986). To estimate absolute values of TEC the uncertainty of phase

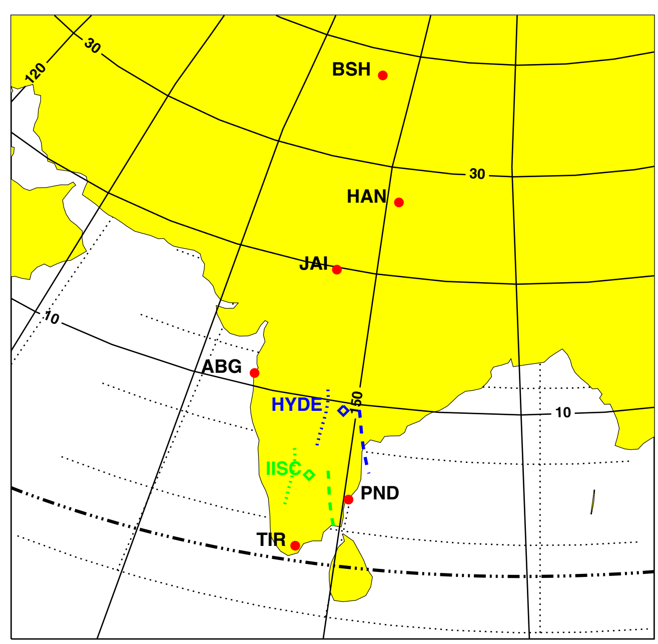

Fig. 1. Map of magnetic stations (red dots) and GPS receivers (empty squares) used in the study in geomagnetic (solid lines) and geographic (dotted lines) coordinates. Dotted-dashed line denotes the geomagnetic dip equator. The ionospheric traces of the pierce points at altitude 300 km are shown for GPS20 satellite during time interval A (0400–0630 UT) with dotted line, and for GPS27 satellite during interval B (1000–1200 UT) with dashed line, for the receivers at HYDE (blue) and IISC (green).

Table 1
Observatories.

Observatory name	IAGA code	Geographic		Geomagnetic		Sampling rate
		Latitude (°N)	Longitude (°E)	Latitude (°N)	Longitude (°E)	
Bishkek	BSH	42.60	74.60	37.9	147.2	20 s
Hanle	HAN	32.76	78.95	23.5	153.3	1 s
Jaipur	JPR	26.92	75.80	18.4	150.2	5 s
Alibag	ABG	18.62	72.87	10.4	146.5	1 min
Pondicherry	PND	11.92	79.92	03.1	152.7	5 s
Tirunelveli	TIR	8.70	77.80	−00.2	150.0	5 s
Indian Institute of Science GPS	IISC	13.02	77.57	04.1	150.1	30 s
Hyderabad GPS	HYDE	17.42	78.55	08.3	151.5	30 s

parameter has been resolved with the use of group delays (Afraimovich and Tatarinov, 2005; Yasjukevich et al., 2013). Commonly there are numerous anomalies in the GPS observational data, and some random errors are known as cycle slips – discontinuities of an integer number of cycles in the measured carrier phase. Though these phase slips caused by the loss of lock in a GPS receiver can be almost totally removed after they are correctly identified (Horvath and Crozier, 2007), there was no need to apply this technique, because during the considered event typical signatures of phase slips – TEC jumps, had not been observed.

We use the standard TEC data with 30-s cadence from the array of GPS receivers at low latitudes in the Indian sector. The GPS receivers operational at Hyderabad (HYDE) and Indian Institute of Science (IISC), Bangaluru, fall in the middle of the magnetometer array (Fig. 1). Dual-frequency GPS method uses the phase information for estimating the slant total electron content N_T in TEC units ($1\ \text{TECu} = 10^{16}\ \text{e/m}^2$). In this study we are interested in periodic TEC variations, whereas absolute values of TEC are not so important. To highlight TEC variations in the Pc5 band we applied a detrending procedure (with a cut-off frequency of 1 mHz) to TEC data.

2.1. Oct. 31, 2003 event

During the 2003 "Halloween storm" the superposition of 3 large magnetic storms occurred during October 29–31, caused by an extremely fast coronal mass ejection. During the recovery phases of these storms very intense (up to several hundred nT) Pc5 waves ($f \sim 3$ mHz) were observed (Marin et al., 2014). In this study we concentrate on global Pc5 event observed on Oct. 31, 2003 (day 304). During this event the global character of Pc5 waves is well pronounced: coherent quasi-monochromatic variations are observed over a wide range of latitudes (Kleimenova and Kozyreva, 2005).

2.2. TEC fluctuations and Pc5 geomagnetic pulsations

During most intense Pc5 activity the wave power was concentrated in the pre-noon and post-noon LT sectors. Magnetometer data from the meridional profile around $\Lambda \sim 150°$ show substorm onset (AE-index up to 1800 nT) at ~01 UT and subsequent intensification of Pc5 activity during intervals: (A) pre-noon 0400–0630 UT, and (B) post-noon 1000–1200 UT. Quasi-monochromatic pulsations can be clearly seen in both H (Fig. 2a) and D (Fig. 2b) horizontal components. Amplitude of pulsations in D component is ~2–3 times smaller than that in H component. Much weaker pulsations are observed in the vertical Z component (not shown). Pulsations are highly coherent throughout the array, from latitude ~40° (Bishkek) up to the geomagnetic equator (Tirunelveli).

During these intervals of enhanced Pc5 activity, TEC fluctuations have been compared with ground geomagnetic variations. Owing to the global character of these waves, a small mismatch between the positions of magnetic station and sub-ionospheric point is not significant. The tracks of vertical projections of intersection with the ionosphere at altitude 300 km of radio paths from satellites GPS20 and GPS27 to ground GPS receivers are shown in Fig. 1. In order to investigate small-scale fluctuations we have detrended raw TEC data with a highpass filter with a cut-off frequency of 1 mHz.

2.2.1. Interval A (0400–0630 UT)

The TEC fluctuations recorded by GPS receivers, HYDE and IISC, have been compared with geomagnetic pulsations (H component) at magnetic station ABG nearly at the same latitude. This comparison (Fig. 3) shows that detrended TEC fluctuations along paths HYDE-GPS20 and IISC-GPS20 look similar to Pc5 pulsations recorded in magnetic data at ABG. The right panel of Fig. 3 is the result of wavelet analysis, which confirms that both fluctuations have the same dominant period $T \sim 5$–6 min. On an average the peak-to-peak amplitudes of oscillations of the TEC are $\Delta N_T \sim 0.3$ TECu and those for magnetic pulsations are $\Delta H \sim 60$ nT.

The cross-spectral analysis (Fig. 4) confirms the presence of identical oscillations in geomagnetic as well as TEC data. The cross spectrum maximizes at the period $T \sim 5$–6 min. Spectral coherence is observed to be high ($\gamma \sim 0.8$) in the vicinity of the cross-spectrum maximum.

Cross-phases $\Delta\phi$ between TEC fluctuations from the HYDE and IISC receivers (GPS20) and magnetometer record at ABG in the spectral domain with high coherency

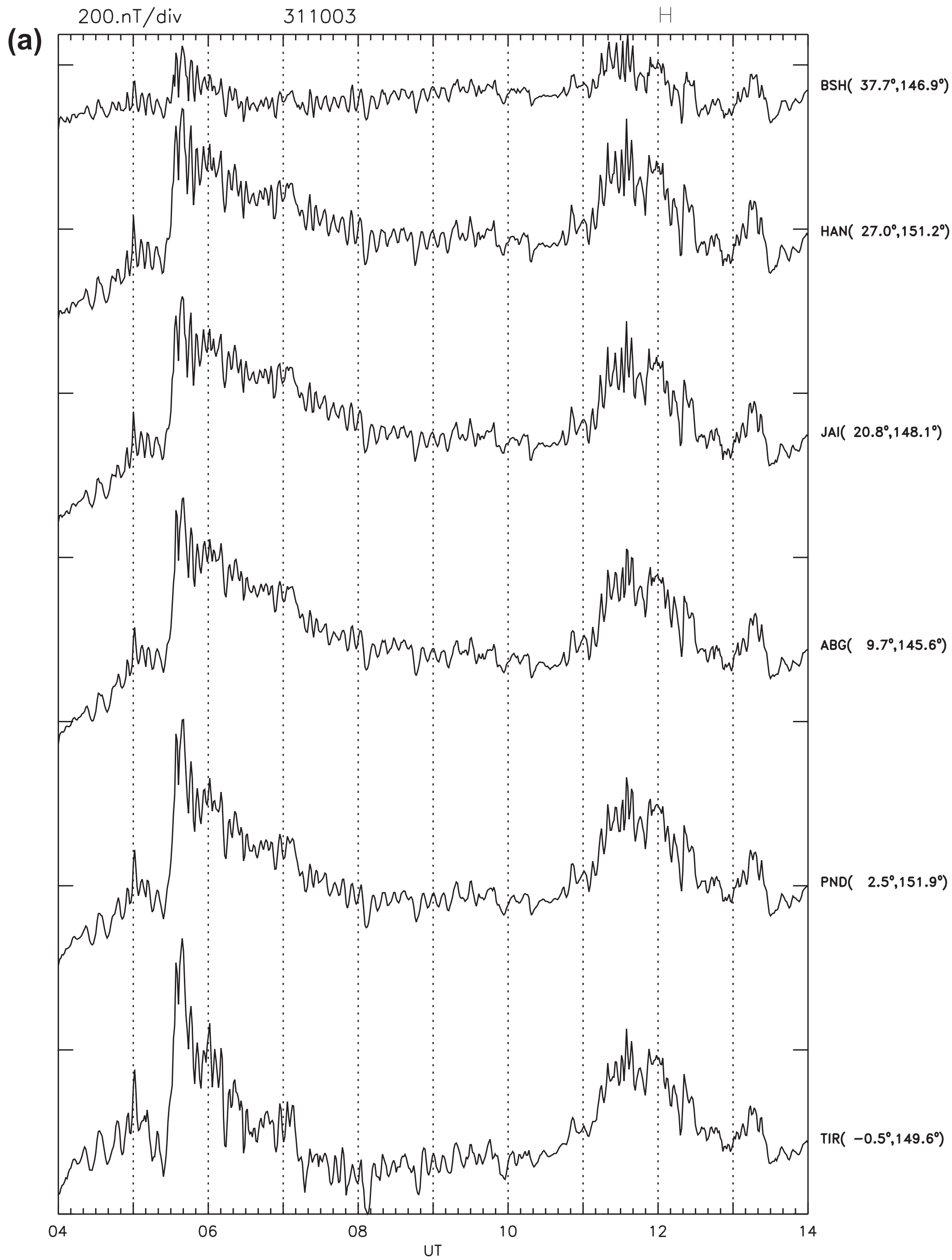

Fig. 2. Magnetometer data from the meridional array along 150° geomagnetic meridian BSH-HAN-JAI-ABG-PND-TIR during the time interval 2003, Oct. 31, 04–14 UT: (a) H-component, and (b) D-component. Geomagnetic coordinates of each station are shown near the right-hand axis.

are less than 30° (Fig. 4). Notice that an estimate of $\Delta\phi$ is reliable only in a spectral domain where power spectra of time series under analysis is high. It seems that TEC fluctuations have a small phase shift in regard to magnetic pulsations. However, a detailed examination of superposed TEC/H variations has shown that the phase delay between them is not very stable, but fluctuates. Thus, realistically, one can just claim that phase difference is closer to 0, than to $\pi/2$.

2.2.2. Interval B (1000–1200 UT)

During this time interval GPS satellites in the vicinity of the IISC receiver are GPS08, GPS27, and GPS07. The comparison of TEC fluctuations along IISC-GPS27 with magnetic variations at ABG shows the occurrence of persistent TEC periodicity nearly on the same time scale as geomagnetic pulsations (Fig. 5). The peak-to-peak amplitudes of oscillations of the TEC are $\Delta N_T \sim 0.2$ TECu and those for magnetic pulsations are $\Delta H \sim 50$ nT. Wavelet

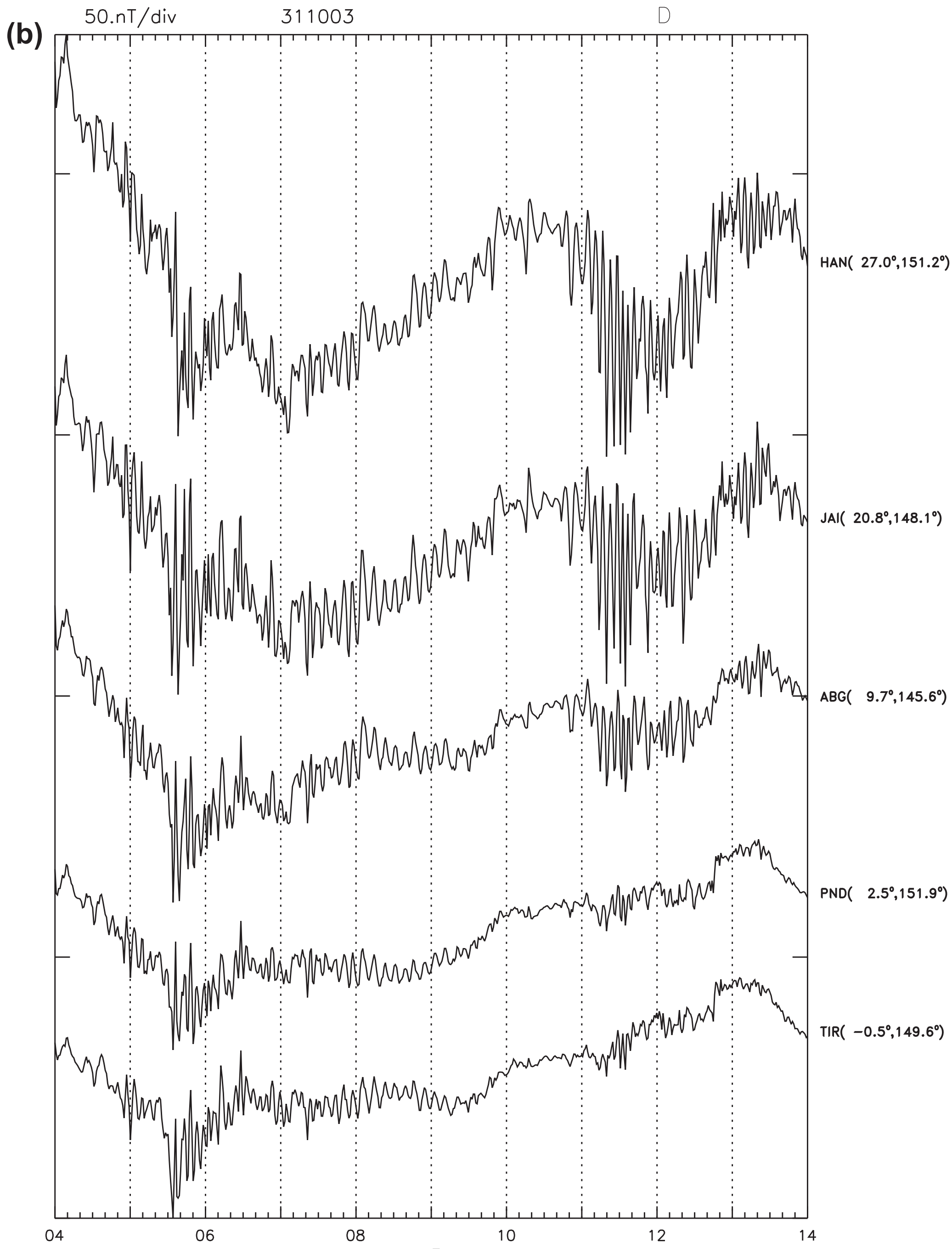

Fig 2. *(continued)*

analysis shows similar wave disturbances in TEC and geomagnetic field variations having periodicity ~4–6 min.

Cross-spectral analysis (Fig. 6) confirms the good correspondence between TEC and magnetic field variations. During the analyzed interval TEC fluctuations and magnetic pulsations have the same $T \sim 4$–6 min. The spectral coherency around this period is also high ($\gamma \sim 0.8$).

Cross-phase angles $\Delta\phi$ between TEC fluctuations from the IISC GPS receivers (GPS27) and magnetometer record at ABG are around 20°. The phase shift between pulsations in H-component of geomagnetic field and TEC fluctuations both for HYDE and IISC receivers is small, though fluctuates noticeably.

3. Plausible theoretical mechanisms

Here, we discuss possible mechanisms which can explain the response of the TEC to ULF pulsations at low latitudes. The temporal variations in the TEC evaluated along the line between a source (S) and receiver (R), N_T, is given by $\partial_t N_T = \int_S^R \partial_t N dz$. Variations of local plasma density

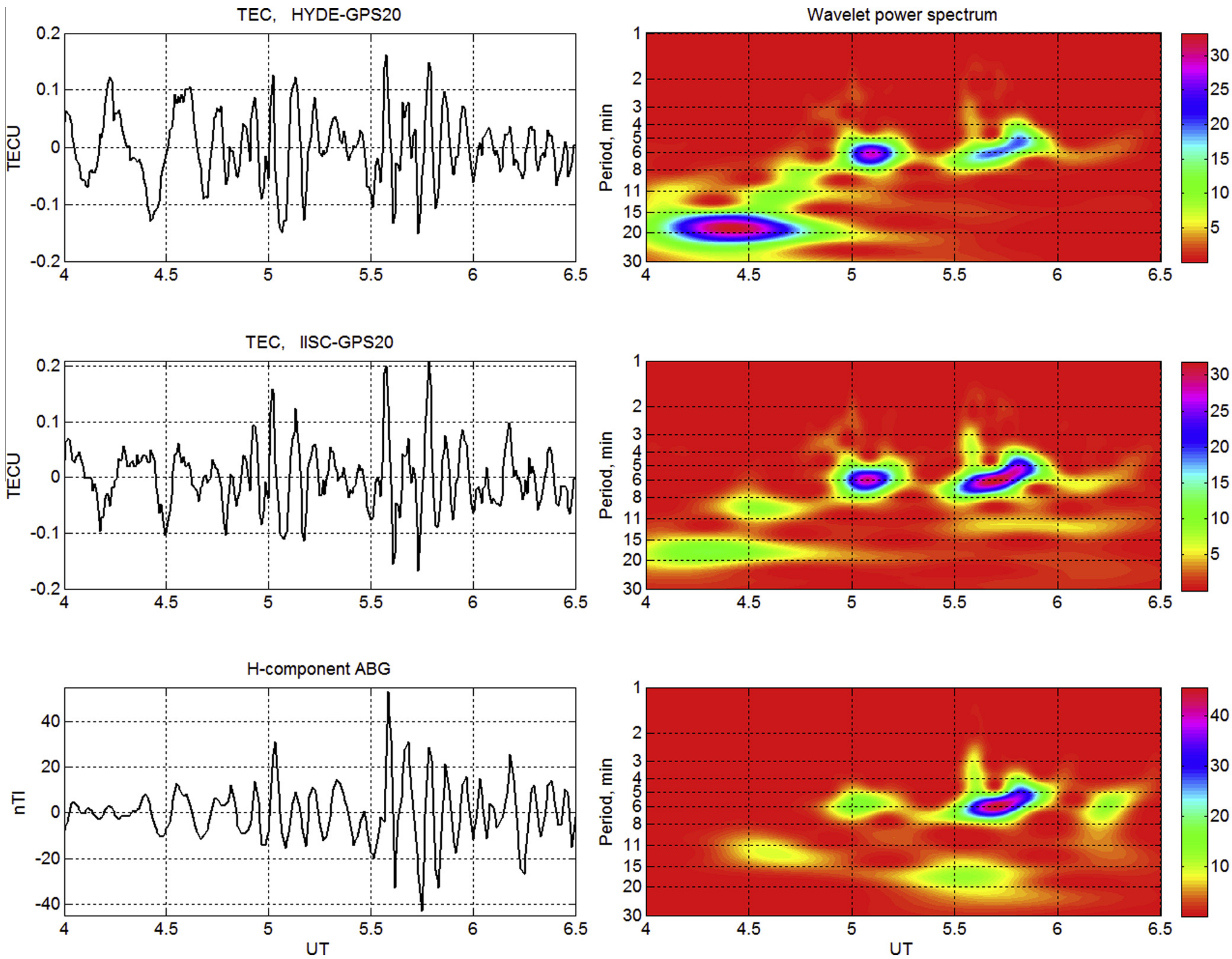

Fig. 3. Comparison of TEC variations (GPS20 satellite) and magnetic variations at station ABG during the time interval *A* (0400–0630 UT): detrended (1 mHz cut-off) TEC variations at receivers HYDE, IISC, and *H*-component magnetic pulsations (left-hand panels); the relevant Morlet wavelet spectra (right-hand panels).

$N(t,z)$ are described by the electron continuity equation (Rishbeth and Garriott, 1964)

$$\partial_t N = -\mathbf{V} \cdot \nabla N - N \nabla \cdot \mathbf{V} + Q - L \quad (1)$$

where Q and L are the electron production and loss rates respectively and $\mathbf{V}$ is the plasma velocity due to the ULF perturbation. In the *F*-layer the recombination rate in (1) is $L = \beta N$, where β is the recombination coefficient. Assuming Q and L are steady, variations in TEC arise from the advection (first right-hand) and divergence (second right-hand) terms. Variations in TEC along the signal path introduce time/phase delays for high frequency radio wave propagation through the ionosphere.

In the "cold" plasma of the upper ionosphere the magnetospheric ULF pulsations are in general a mixture of Alfven and compressional fast magnetosonic (FMS) waves. At high latitudes, numerous ground, satellite, and radar observations demonstrated that Pc5 waves in the ionosphere are predominantly composed of Alfven waves. However, the transmission of global Pc5 waves to lower and equatorial latitudes most probably is provided by some non-Alfvenic mechanism, e.g., cavity mode or MHD waveguide mode. Therefore, it seems more realistic to examine the TEC response at low latitude to FMS mode. In the considered event, no noticeable riometer variations were observed. Though riometer data can detect the periodic precipitation of energetic electrons with energies >30 keV, the possibility of low-energy electron (<10 keV) precipitation remains unclear.

3.1. Ground magnetic signature due to FMS mode

We suppose that Pc5 waves in the low-latitude topside ionosphere are mostly the manifestation of FMS mode. This mode is easily identified in space by the disturbed total magnetic field $|B|$ or field-aligned component $B_{\|}$. However, both azimuthally large-scale Alfven and FMS magnetospheric modes mainly contribute to the *H*-component on the ground. Therefore, for the interpretation of the coordinated TEC-magnetometer observations we have to consider the FMS wave interaction with the multi-layered system i.e. magnetosphere – thin ionosphere – non-conductive atmosphere – ground. For ULF waves with period $T > 10$ s, the width of the conductive E-layer is much smaller than the wavelength and hence the E-layer can be replaced by an infinitesimally thin sheet with height-integrated Pedersen and Hall conductances $\sum_P$ and $\sum_H$ at the ionospheric altitude h. We assume that X-coordinate corresponds to the North–South (radial) direction, and Y corresponds to the East–West (azimuthal) direction. Magnetic field is inclined by angle I to the Earth's surface. Here, we use some theoretical concepts from the thin sheet approximation of the MHD wave theory (Alperovich and Fedorov, 2007).

The wave scale of the FMS mode in the Pc5 range in the magnetosphere is very large. Therefore, FMS waves cannot reach the bottom ionosphere directly, especially at low latitudes, under reasonable horizontal wave numbers, $k_z \sim 1/3R_E$, $k_y \sim 1/(5-10)R_E$. Indeed, as follows from the dispersion relationship, the radial wave number $k_x = \sqrt{\omega^2/V_A^2(x) - k_z^2 - k_y^2}$ upon wave propagation towards plasma with a higher V_A becomes imaginary, which means a non-propagation (opaque) region where the wave becomes evanescent. An exact location of the cut-off surface is hard to estimate analytically. In reality, the spatial distribution of wave power is determined by the diffraction of an incident large-scale FMS mode on a relatively small conductive sphere (Earth). However, because of its large horizontal coverage, even an evanescent fast mode can convey significant wave energy towards the Earth.

In order to estimate the magnetic field compression in the upper ionosphere we apply a theoretically predicted amplitude ratio and phase delay $\Delta\phi$ between the ground magnetic signal $B_x^{(g)}$ and the tangential magnetic component $B_\tau = B_\| \cos I$ (at near-equatorial latitudes $B_\tau \approx B_\|$) of the incident FMS wave at the ionospheric height. These relationships are determined by the transmission properties of the whole ionosphere–atmosphere–ground system. The thin ionosphere theory (Pilipenko et al., 2011) provides a remarkably simple relationship between the magnetic disturbance in the ionosphere and its ground response for a highly-conductive ground ($\sigma_g \to \infty$) as follows:

$$\left|\frac{B_\tau}{B_x^{(g)}}\right| = \sqrt{1+p^2}, \quad \Delta\phi = -tan^{-1}p, \quad p = \frac{\omega h}{V_C} \qquad (2)$$

Here, $V_C = (\mu_o \Sigma_C)^{-1}$ is the ionospheric Cowling velocity, determined by the Cowling ionospheric conductance $\Sigma_C = \Sigma_P + \Sigma_H^2/\Sigma_P$. For approximate estimates, one can use the relation $V_C[\text{km/s}]\| \simeq 800/\Sigma_C[\text{S}]$. The parameter p controls the penetration of the FMS mode through the ionosphere to the ground. According to (2), the phase delay

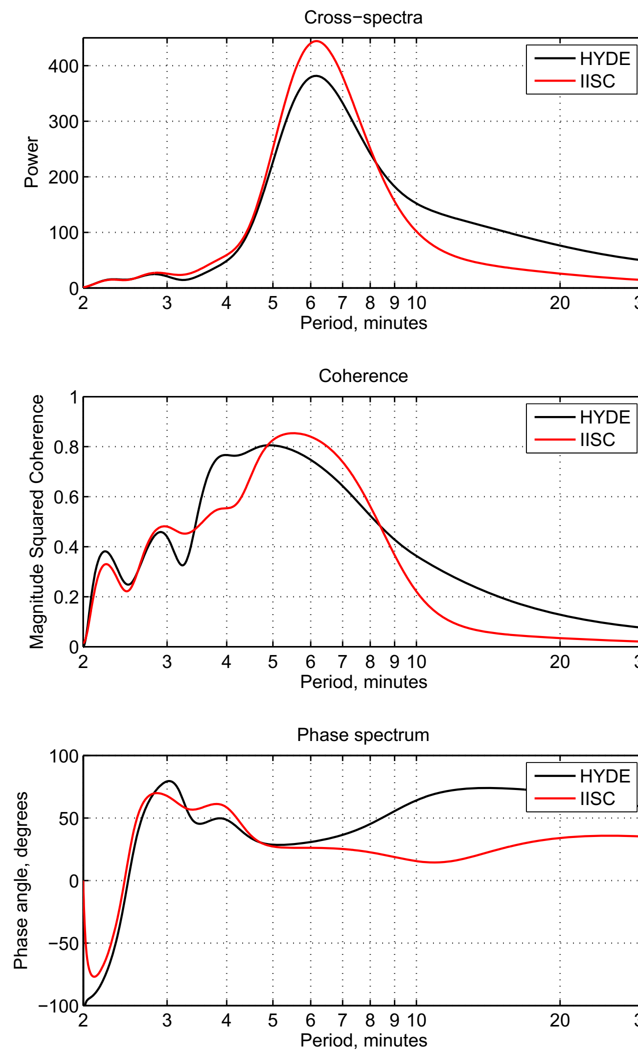

Fig. 4. Cross-spectral analysis of TEC variations (GPS20 satellite) recorded at HYDE and IISC receivers and magnetic variations (H-component) at station ABG during the time interval A (0400–0630 UT): amplitude cross-spectrum $S(T)$ (upper panel), squared spectral coherence $\gamma(T)$ between TEC and magnetic variations (middle panel), and cross-phase $\Delta\phi(T)$ (bottom panel).

between topside ionosphere and ground must increase with wave frequency ω as well as the ionospheric conductance $\sum_C$.

The Pc5 observational period corresponds to the daytime conditions. For typical dayside parameters $\sum_H = 20$ S, $\sum_P = 10$ S, resulting into $\sum_C = 50$ S, and $V_C = 16$ km/s. For waves with $\omega = 0.02\ \text{s}^{-1}$, the parameter p has the value of $\sim$0.15. Therefore, the ratio of a signal amplitude in space and on the ground is $\sim$1.0 and the phase shift produced by the ionosphere is $\Delta\phi \sim 10°$. Thus, the ionosphere may be considered as nearly transparent for FMS mode at low latitude during typical day time conditions.

The electric field in the ionosphere induced by FMS mode can be estimated assuming a low-absorbing ionosphere. The N–S component of the magnetic field $B_x^{(g)}$ on

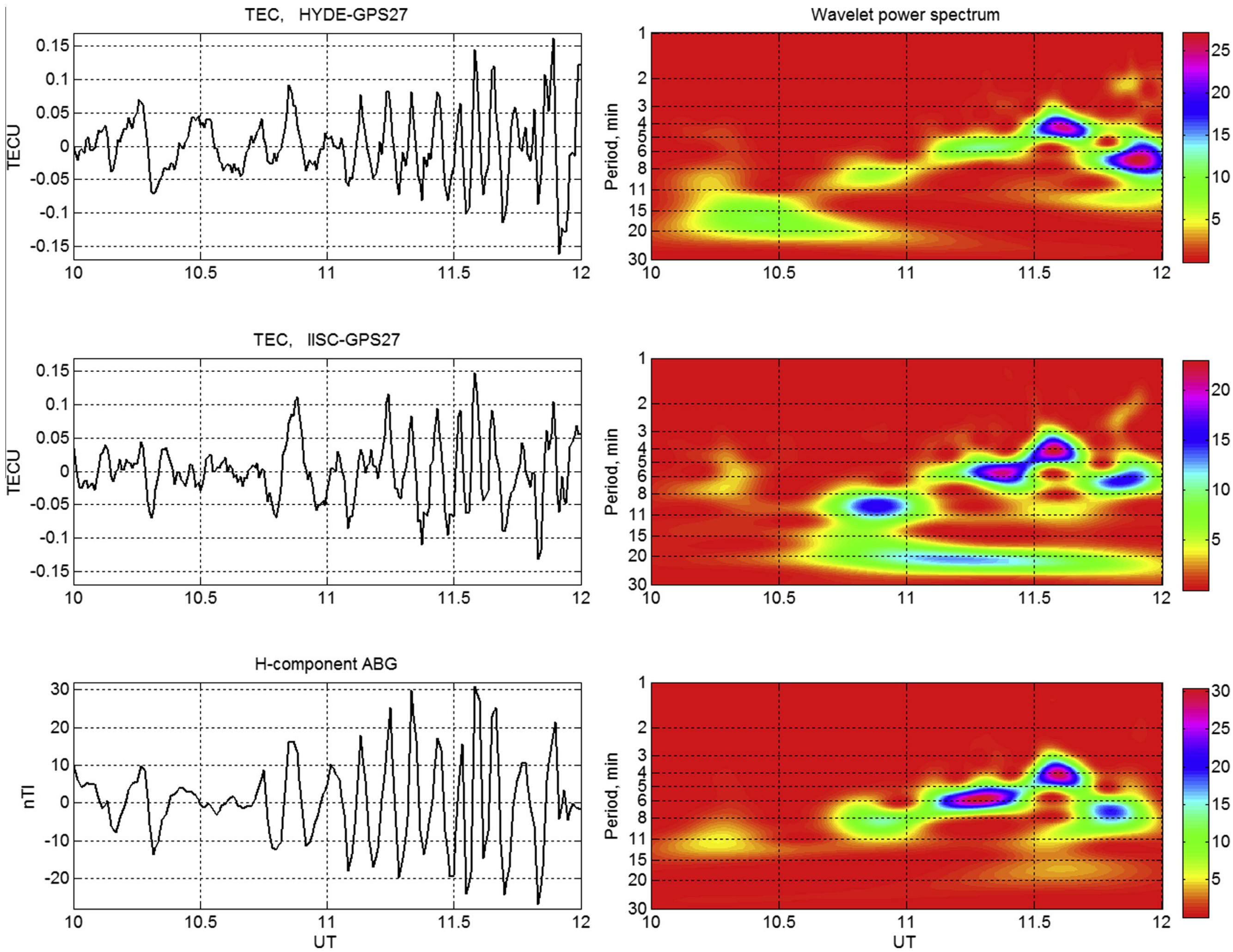

Fig. 5. Comparison of TEC variations (GPS27 satellite) and magnetic variations at station ABG during the time interval *B* (1000–1200 UT): detrended TEC variations at receivers HYDE, IISC, and *H*-component magnetic pulsations (left-hand panels); the relevant Morlet wavelet spectra (right-hand panels).

the ground and the *E–W* component of the electric field $E_y(z)$ in the ionosphere at an altitude z_h above the ground with impedance Z_g, produced by a FMS wave, are related by (Teramoto et al., 2014)

$$E_y(z)/B_x^{(g)} = -i\omega z_h + Z_g/\mu_0 \quad (3)$$

The second term in the right-hand side of (3) corresponds to the effect of the finite ground conductivity. According to (3), for a FMS wave with magnetic component on the ground as 50 nT, the magnitude of electric field at altitude 300 km $|E_y|$ is ~0.3 mV/m. Thus, FMS mode waves would induce a rather weak electric field in the ionosphere.

3.2. TEC modulation by FMS mode

Two mechanisms might be responsible for the TEC modulation by FMS mode. The finite East–West E_y component of the incident FMS wave causes a vertical plasma drift $V_z = E_y \cos I/B_o$, where B_0 is the ambient geomagnetic field. Owing to the strong altitude dependence of ionization $Q(z)$ and recombination $L(z)$ rates, the vertical shift causes a plasma modification due to the changes of ionization–r ecombination balance (Poole and Sutcliffe, 1987). For Pc5 with $\omega \sim 0.02\ s^{-1}$, $\beta \sim 10^{-4}\ s^{-1}$, V_z[m/s] ~ 20E[mV/m]cos$I$, cos$I$ ~ 0.9, and E ~ 0.3 mV/m, the estimate of this mechanism gives $\Delta N/N \sim 0.005\%$. This estimate shows that the electric field perturbation associated with FMS wave can hardly explain the TEC response to geomagnetic Pc5 oscillations.

Other possibility is that the TEC modulation may be related to the plasma/magnetic compression in a FMS wave. The plasma oscillations in this mode are about of the same relative amplitude as oscillations of the magnetic field, that is $\Delta N_T/N_T \sim \Delta N/N = \Delta B/B$. The consideration in the previous section has shown that compressional magnetic component in the ionosphere and ground horizontal magnetic component are nearly the same in magnitude. Absolute values of vTEC during the considered event was determined to vary around 80 TECu (Fig. 7). This

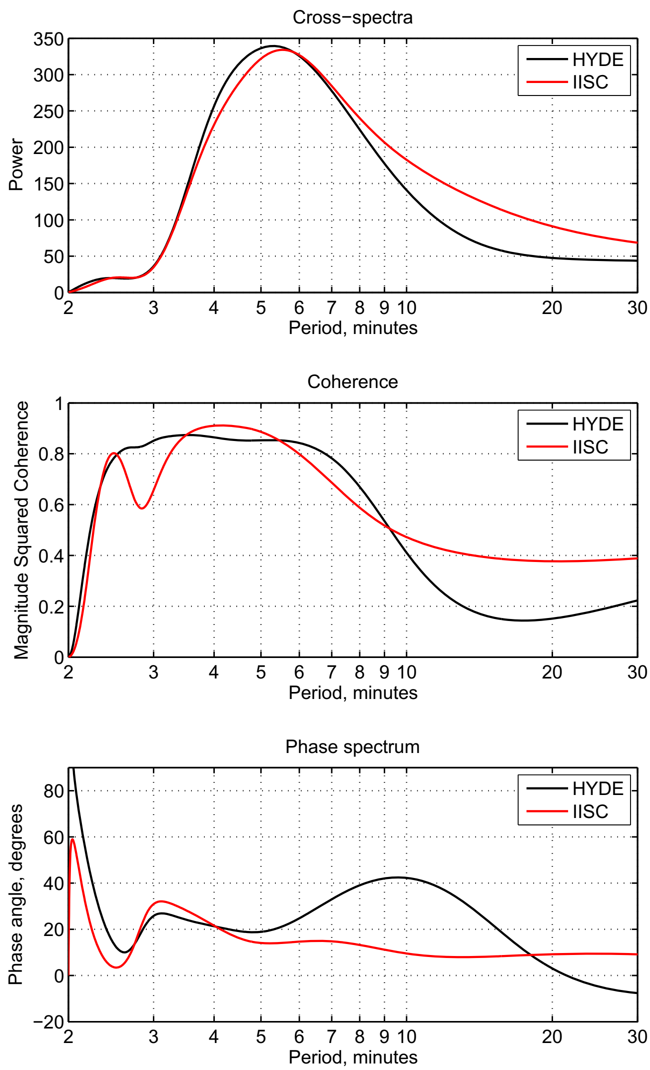

Fig. 6. Cross-spectral analysis of TEC variations (GPS27 satellite) recorded at HYDE and IISC receivers and magnetic variations (H-component) at station ABG during the time interval B (1000–1200 UT): amplitude cross-spectrum $S(T)$ (upper panel), squared spectral coherence $\gamma(T)$ between TEC and magnetic variations (middle panel), and the cross-phase $\Delta\phi(T)$ between them (bottom panel).

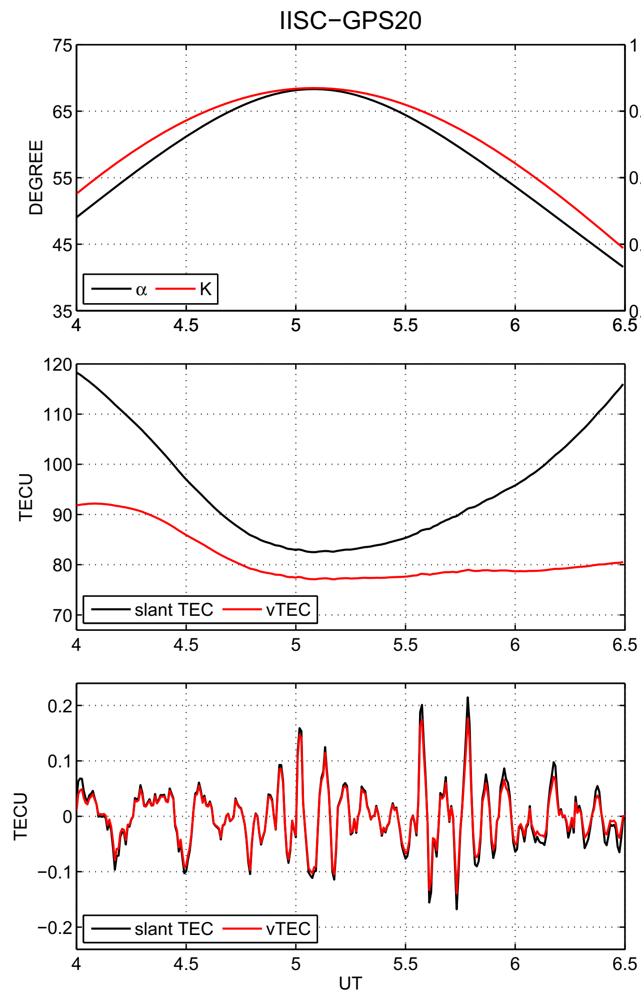

Fig. 7. Variations during the event of the elevation angles α and correction factor K (upper panel); slant and vertical TEC (middle panel), and superposed vTEC and slant TEC fluctuations (bottom panel).

value, observed during the storm period, is larger than the value given for the given location by the IRI model (by numerical integration from 50 to 2000 km) (Bilitza et al. 2011): at 06 UT, $\sum_P \approx 20.4$ S, $\sum_H \approx 22.0$ S, and $N_T \approx 45.8$ TECu; whereas at 11 UT, $\sum_P \approx 21.6$ S, $\sum_H \approx 12.8$ S, and $N_T \approx 55.3$ TECu. The elevation angles during the event changed from $\alpha = 35°$ till $\alpha = 70°$, whereas the correction factor varied from ~0.5 till ~0.9. The variation of α was accompanied by variations of slant TEC. However, amplitude of vTEC periodic fluctuations was just ~10% smaller than that of slant TEC fluctuations (Fig. 7).

For a typical peak-to-peak amplitudes of TEC oscillations $\Delta N_T \sim 0.2$ TECu, and magnetic pulsations $\Delta H \sim 50$ nT, the ratio between the TEC and H-component magnetic variations is $\Delta N_T/\Delta H \sim 4 \cdot 10^{-3}$ TECu/nT. Assuming that at the F-layer of the ionosphere $B_o = 25{,}000$ nT, Pc5 geomagnetic pulsations with amplitude 50 nT produce ~0.2% modulation of the geomagnetic field in the upper ionosphere. Simultaneous pulsations of TEC with 0.2 TECu amplitude, for $N_T = 80$ TECu, correspond to the observed TEC modulation of ~0.25%. Thus, the TEC response to global Pc5 waves has turned out to be nearly the same as the geomagnetic field modulation. However, any conclusive mechanism for TEC modulation by ULF waves can be established only after more detailed studies using other ionospheric instruments which will provide comprehensive information about ionospheric plasma parameters.

4. Discussion: significance of combined TEC-magnetometer observations at low latitudes

Long-period pulsations are the most powerful wave processes in the terrestrial environment and they can significantly modulate the magnetospheric and ionospheric plasma. The radar community has demonstrated that Pc5 waves can modulate the ionospheric electric field and plasma convection velocity, field-aligned current, electron density, the ionospheric conductance and electron and ion temperatures in both *F*- and *E*-layers (see references in Pilipenko et al. (2014b)). Recent observations have confirmed that Pc5 waves can cause periodic TEC modulation as well (Pilipenko et al., 2014a; Watson et al., 2015). Moreover, as has been demonstrated in this paper, the ULF modulation effects can be observed not only at auroral, but at low latitudes as well. Here we have shown data from GPS satellites with pierce points nearest to the magnetometer location. But, periodic TEC variations related to global Pc5 waves were seen in signals from other GPS satellites above the Indian sub-continent: For the interval A: 02, 07, 08, 20, 27; and for the interval B: 07, 08, 23, 27. However, because of the paper size limitations, we cannot demonstrate all the data.

The combined TEC-magnetometer observations at low latitudes provide important information about the physical nature of global Pc5 waves. The presented observational results on TEC modulation by Pc5 waves at low latitudes cannot be interpreted on the basis of the Alfven mode concept and rather support the mechanism of MHD waveguide excitation. According to Marin et al. (2014), the large latitudinal coverage of Pc5 pulsations during the Oct. 31 event is due to the excitation of MHD waveguide mode, trapped between the magnetopause and the equatorial ionosphere. Surprisingly deep penetration of global Pc5 wave power to low latitudes is probably related to the radial structure of Alfven velocity $V_A(L)$ across L-shells during strong magnetic storms. During moderate geomagnetic activity, the reflection point of the waveguide mode is in the vicinity of the plasmapause, where a steep gradient of $V_A(L)$ occurs. During strong magnetic storms, probably due to a significant contribution of oxygen ions into the magnetospheric plasma content, this gradient is smoothed and the reflection point shifts to the equatorial ionosphere. The frequency of the waveguide mode is determined by the radial scale of the waveguide and averaged Alfven velocity. Upon reflection of FMS mode from the ionosphere a node for radial plasma displacement and anti-node of compressional component is to be formed in this region (Takahashi et al., 1995). This structure is reflected in the ground latitudinal structure of the H-component with a peak at the equator. Estimate of the fundamental quarter-wavelength FMS mode (with anti-node at the ionosphere and node at the magnetopause) matches the frequency of observed Pc5 pulsations assuming $V_A \sim 400$ km/s. Such low magnitude of the Alfven velocity is due to the dominance of $O+$ ions in the magnetosphere during the recovery phase of strong magnetic storms.

FMS waveguide mode reaching the low-latitude ionosphere causes both periodic modulation of TEC and magnetic response on the ground. The estimated maximum percentage change in TEC by this mechanism is found to be approximately the same as the observed value in the frameworks of a simple model with a vertical radiopath. More adequate quantitative interpretation of TEC oscillation, comprising a dependence on elevation angle α, demands an advanced 2D model which should take into account a realistic geometry of the geomagnetic field, wave spatial structure, and satellite-receiver path orientation. Probably, during observations under small α some additional averaging of the TEC modulation effect will be introduced.

The ground data on ULF field can be used to estimate the disturbed electric and magnetic field in the ionosphere with a reasonable accuracy using a well-justified model. Our observations have shown that in order to produce ~0.1 TECu disturbance with time scale ~1–10 min at low latitudes the magnetic field compression ~20 nT is necessary. Therefore, there is a feasibility of using this information as a calibration experiment to evaluate the ionospheric response to an external forcing with unknown parameters, such as seismic activity before and after shock, distant atmospheric and underground explosions, hurricanes and thunderstorms, etc.

5. Conclusion

The GPS/TEC technique has turned out to be sensitive enough to detect intense Pc5 waves even at low latitudes. Combined usage of magnetometer and GPS/TEC data is a very promising way to reveal the physical mechanism of disturbances. Relative TEC disturbance induced by global Pc5 waves is almost the same as that of the magnetic field. Theoretical estimates of the mechanism of the plasma compression by FMS mode gives reasonable magnitudes of the expected TEC modulation depth. Despite this, the effect of TEC modulation by ULF waves is a challenge for the MHD wave theory because the responsible mechanism of such modulation has not been firmly established yet.

Acknowledgements

This study was supported by the Russian Foundation for Basic Research Grants 15-05-01814 (EV), 13-05-90436 (EF), and 15-55-45064 (VP,AS,GV). We appreciate the help of O. Kozyreva, and thorough reading and useful comments of both Reviewers. Dual-frequency 30-s rate GPS measurements are freely available as daily data files in RINEX format from the IGS (ftp://cddis.gsfc.nasa.gov).

References

Afraimovich, E.L., Tatarinov, P.V., 2005. Reconstruction of total electron content on a basis of data from dual-frequency GPS-receiver based onboard low earth orbiter. Investigated Russia 042, 474–481.

Afraimovich, E.L., Astafyeva, E.I., Demyanov, V.V., et al., 2013. A review of GPS/GLONASS studies of the ionospheric response to natural and anthropogenic processes and phenomena. J. Space Weather Space Clim. 3, A27.

Alperovich, L.S., Fedorov, E.N., 2007. Hydromagnetic waves in the magnetosphere and the ionosphere. Astrophysics and Space Science Library, vol. 353, XXIV, p. 418, ISBN:978-1-4020-6636-8.

Bilitza, D., McKinnell, L.-A., Reinisch, B., Fuller-Rowell, T., 2011. The international reference ionosphere (IRI) today and in the future. J. Geod. 85, 909–920.

Galvan, D.A., Komjathy, A., Hickey, M.P., Mannucci, A.J., 2011. The 2009 Samoa and 2010 Chile tsunamis as observed in the ionosphere using GPS total electron content. J. Geophys. Res. 116, A6. http://dx.doi.org/10.1029/2010JA016204.

Davies, K., Hartman, G.K., 1976. Short-period fluctuations in total columnar electron content. J. Geophys. Res. 81, 3431–3434.

Fitzgerald, T.J., 1997. Observations of total electron content perturbations on GPS signals caused by a ground level explosion. J. Atmos. Sol.-Terr. Phys. 59, 829–834.

Hamada, A.M., Mahrous, A.M., Fathy, I., Ghamry, E., Groves, K., Yumoto, K., 2015. TEC variations during geomagnetic storm/substorm with Pc5/Pi2 pulsation signature. Adv. Space Res. 55, 2534–2542.

Hofmann-Wellenhof, B., Lichtenegger, H., Collins, J., 1992. Global Positioning System: Theory and Practice. Springer-Verlag Wien, New York.

Horvath, I., Crozier, S., 2007. Software developed for obtaining GPS-derived total electron content values. Radio Sci. 42, RS2002. http://dx.doi.org/10.1029/2006RS003452.

Kleimenova, N.G., Kozyreva, O.V., 2005. Spatial–temporal dynamics of Pi3 and Pc5 geomagnetic pulsations during the extreme magnetic storms in October 2003. Geomagn. Aeron. (Engl. Transl.) 45, 71–79.

Klobuchar, J.A., 1986. Ionospheric time-delay algorithm for single-frequency GPS users. IEEE Trans. Aerosp. Electron. Syst. 23, 325–331.

Komjathy, A., Galvan, D.A., Stephens, P., et al., 2012. Detecting ionospheric TEC perturbations caused by natural hazards using a global network of GPS receivers: the Tohoku case study. Earth Planets Space 64, 1287–1294.

Liu, J.Y., Chuo, Y.J., Shan, S.J., Tsai, Y.B., Chen, Y.I., Pulinets, S.A., Yu, S.B., 2004. Pre-earthquake ionospheric anomalies registered by continuous GPS TEC measurements. Ann. Geophys. 22, 1585–1593.

Marin, J., Pilipenko, V., Kozyreva, O., Stepanova, M., Engebretson, M., Vega, P., Zesta, E., 2014. Global Pc5 pulsations during strong magnetic storms: excitation mechanisms and equatorward expansion. Ann. Geophys. 32, 319–331.

Menk, F.W., Waters, C.L., Dunlop, S.I., 2007. ULF Doppler oscillations in the low latitude ionosphere. Geophys. Res. Lett. 34, L10104. http://dx.doi.org/10.1029/2007GL029300.

Motoba, T., Kikuchi, T., Luehr, H., Tachihara, H., Kitamura, T.-I., Hayashi, K., Okuzawa, T., 2002. Global Pc5 caused by DP2-type ionospheric current system. J. Geophys. Res. 107. http://dx.doi.org/10.1029/2001JA900156.

Pilipenko, V., Fedorov, E., Heilig, B., Engebretson, M.J., Sutcliffe, P., Luehr, H., 2011. ULF waves in the topside ionosphere: satellite observations and modeling. The Dynamic Magnetosphere. In: Liu, W., Fujimoto, M. (Eds.), . IAGA Special Sopron Book Series, vol. 3. Springer (Chapter 14, pp. 257–269).

Pilipenko, V., Belakhovsky, V., Murr, D., Fedorov, E., Engebretson, M., 2014a. Modulation of total electron content by ULF Pc5 waves. J. Geophys. Res. 119, 4358–4369.

Pilipenko, V., Belakhovsky, V., Kozlovsky, A., Fedorov, E., Kauristie, K., 2014b. ULF wave modulation of the ionospheric parameters: radar and magnetometer observations. J. Atmos. Sol.-Terr. Phys. 108, 68–76.

Poole, A.W.V., Sutcliffe, P.R., 1987. Mechanisms for observed total electron content pulsations at mid latitudes. J. Atmos. Terr. Phys. 49, 231–236.

Potapov, A., Guglielmi, A., Tsegmed, B., Kultima, J., 2006. Global Pc5 event during 29–31 October 2003 magnetic storm. Adv. Space Res. 38, 1582–1586.

Rae, I.J., Donovan, E.F., Mann, I.R., Fenrich, F.R., Watt, C.E.J., Milling, D.K., Lester, M., Lavraud, B., Wild, J.A., Singer, H.J., Rème, H., Balogh, A., 2005. Evolution and characteristics of global Pc5 ULF waves during a high solar wind speed interval. J. Geophys. Res. 110, A12211. http://dx.doi.org/10.1029/2005JA011007.

Rishbeth, H., Garriott, A.K., 1964. Relationship between simultaneous geomagnetic and ionospheric oscillations. Radio Sci. 68D, 339–343.

Saito, A., Fukao, S., Miyazaki, S., 1998. High resolution mapping of TEC perturbations with the GSI GPS Network over Japan. Geophys. Res. Lett. 25, 3079–3082.

Skone, C., Nicholson, N., 2006. Detection and mitigation of geomagnetic pulsation effects using GPS. In: ION GNSS 2006, Session D3, Fort Worth, Texas.

Sinha, A.K., Pathan, B.M., Rajaram, R., Rao, D.R.K., 2001. Low frequency modulation of transionospheric radiowave amplitude at low-latitudes: possible role of field line oscillations. Ann. Geophys. 19, 1–12.

Spanswick, E., Donovan, E., Baker, G., 2005. Pc5 modulation of high energy electron precipitation: particle interaction regions and scattering efficiency. Ann. Geophys. 23, 1533–1542.

Takahashi, K., Ohtani, S., Anderson, B.J., 1995. Statistical analysis of Pi2 pulsations observed by the AMPTE CCE spacecraft in the inner magnetosphere. J. Geophys. Res. 100, 21929–21941.

Teramoto, M., Nishitani, N., Pilipenko, V., Ogawa, T., Shiokawa, K., Nagatsuma, T., Yoshikawa, A., Baishev, D., Murata, K.T., 2014. Pi2 pulsation simultaneously observed in the E and F region ionosphere with the SuperDARN Hokkaido radar. J. Geophys. Res. 119, 3444–3462.

Tsai, H.-F., Liu, J.-Y., Lin, C.-H., Chen, C.-H., 2011. Tracking the epicenter and the tsunami origin with GPS ionosphere observation: Taiwan analysis. Earth Planets Space 63, 859–862.

Tsugawa, T., Otsuka, Y., Coster, A.J., Saito, A., 2007. Medium-scale traveling ionospheric disturbances detected with dense and wide TEC maps over North America. Geophys. Res. Lett. 34, L22101. http://dx.doi.org/10.1029/2007GL031663.

Van de Kamp, M., Pokhotelov, D., Kauristie, K., 2014. TID characterized using joint effort of incoherent scatter radar and GPS. Ann. Geophys. 32, 1511–1532.

Waters, C.L., Yeoman, T.K., Sciffer, M.D., Ponomarenko, P., Wright, D. M., 2007. Modulation of radio frequency signals by ULF waves. Ann. Geophys. 25, 1113–1124.

Watson, C., Jayachandran, P.T., Singer, H.J., Redmon, R.J., Danskin, D. W., 2015. Large-amplitude GPS TEC variations associated with Pc5–6 magnetic field variations observed on the ground and at geosynchronous orbit. J. Geophys. Res. 120. http://dx.doi.org/10.1002/2015JA021517.

Yasjukevich, Yu.V., Edemsky, I.K., Perevalova, N.P., Polyakova, A.S., 2013. Response of the ionosphere on helio- and geophysical disturbances according to the GPS data. Irkutsk, p. 259, ISBN 978-5-9624-0879-8 (in Russian).

Zakharenkova, I.E., Shagimuratov, I.I., Tepenitzina, N.Yu., Krankowski, A.I., 2008. Anomalous modification of the ionospheric total electron content prior to the 26 September 2005 Peru earthquake. J. Atmos. Sol.-Terr. Phys. 70, 1919–1928.